Analysis of Transmitting Rain-Images Based on Polar Codes (Encoder –Decoder) Under Additive White Gaussian Noise

Ibrahim Beram Jasim[#1]

Dept. Of computer technical Engineering, alqalam college unversity, karkuk, Iraq.
Ibrahim.jasim@alqalam.edu.iq

ABSTRACT

The most difficult in computer vision applications is removing white noise and rain in image. White noise and rain frequently coexist in real-world road photographs, but traditional imaging technologies are incapable of resolving this issue. However, we proposed a network based on framework with three step distinct Image decomposition using guided filters and white noise based on polar codes and rainfall removal network, since restoring an image based on a model of atmospheric scattering using expected transmit and received plans and predicted rain removed images technique. Investigational results establish that our trained framework outperforms better design approaches on synthetic and real-world way to test rain-images. We quantitatively evaluate our model using peak signal-to-noise indicators, demonstrating that our methods have the highest PSNR values. However, the design proposed to demonstrate that our method is applicable to real world vision applications based on polar codes (encoder and decoders).

Keywords: Encoder-decoder polar codes, dilated polar codes; image restoration; List decoding, additive white Gaussian noise

1-Introduction

Restoring images that have been damaged by weather to their original, high-quality state is essential for many types of outdoor vision systems, including object detection [1], code length image effect on image-quality, extending the code length possibly will help a little fill the performance polar codes. This is because of the impact of code-length on image quality.[2]

The majority of these vision systems have their designs centered on favorable weather conditions and are intended to function effectively in such environments. However, in the real world, different weather conditions, such as rain and fog, can degrade the camera's input images and the vision system's performance [3]. When it is raining and foggy outside, rain streak occludes adjacent items, and generates AWGN effects with light dispersion, which together reduce both the visibility of objects and the effectiveness of vision systems. Rain streak occludes nearby objects.

An example of using an object detection algorithm on an image of a road that is obscured by fog and rain is presented in figure 1. An inaccuracy in object detection takes place in the image of the muddy and rainy road. There have been many different ideas put forward for recovering photographs that have been ruined by rain[4]. In the past, the primary emphasis was placed on restoration through the use of hand-crafted components. Restoration has mostly been investigated by scholars more recently through the use of neural networks. Research on the removal of rain can be broken down into the following categories:

Getting rid of rain from a single image Getting rid of rain from a single photograph has proven to be a difficult issue because of the lack of data present in comparison to the video based solutions. In spite of these challenges, a wide variety of approaches that involve hand-crafted components have been researched[5].

A straightforward patch-based priors method that makes use of Gaussian mixture models was proposed by Li et al. [6]. These priors are flexible enough to account for rain streaks in a variety of orientations and scales.

Figure 1: Rain image transmit on channel using polar code under AWGN

For instance, Kim et al. [7] suggested a rain line subtraction based region detection technique. This approach examines the elliptical kernel aspect ratio and the rotation angle of the at each point in pixel position. It then applies non-local mean filtering to rain streak regions that have been found. For instance, Fu et al. [8] initially suggested a deep learning-based rain streak removal approach called DerainNet. They subsequently modified the model [9] by applying ResNet structure to lower the mapping range, which resulted in better convergence of loss functions. The authors of [10] .'s study developed a novel model for the rain streak image, which efficiently erased rain streaks by adding a rain region layer.

Rain streaks have been shown to have an effect on X and Y gradients, which led the author in [11] to suggest a method that operates in the gradient domain. However, the removal of rain using simply hand-crafted procedures is not entirely resilient due to the poorly articulated challenge. Recent research has focused on investigating potential solutions to this issue that are based on deeplearning [12]. It has been demonstrated that image transmitted based on succesive cancelation list (SCL) decoders when used polar-codes is superior to low density parity check code when used to Additive White Gausian Noise channels in terms of both throughput and error rate[5]. The proposed the performance of POLAR[14][15] codes versus he Bose–Chaudhuri_Hocquenghem codes (BCH) for rainimage sending using the 64-quadirature amplitude modiulation in OFDM system concluded a constant Additive WGN guide channel with successive cancellation list decodes however the standards of SNR in between five dB to twenty dB, which are considered to be high signal to noise ratio, the polar code when used concatenation technique with a parity check code is also proposed in [2]. It is demonstrated to enhance performance when compared with the practice when using polar codes, although this improvement comes at the expense of a reduction in the overall coding rate[14].

2- Proposed transmitting raining image by using polar codes

Polar codes are linears-blocks codes using two binary (N; K) codes that depend on on the correct selection of K-bitchannels from surrounded by N-bitchannels to construct a codewords however as a result, to convey datawords at a rate that is equal to R times K to the Nth power. The values zero are written into the other K-bit-channel. The particular design that is utilized during the process of constructing the polar code determines the manner in which the bit-channels are selected (Arikan, 2009)[14]. Figure 2 depicts the fundamental format that is utilized for polar codes.

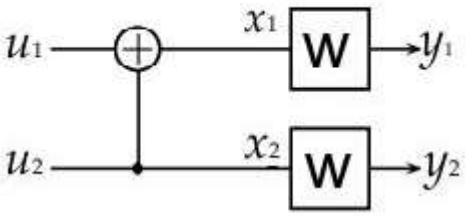

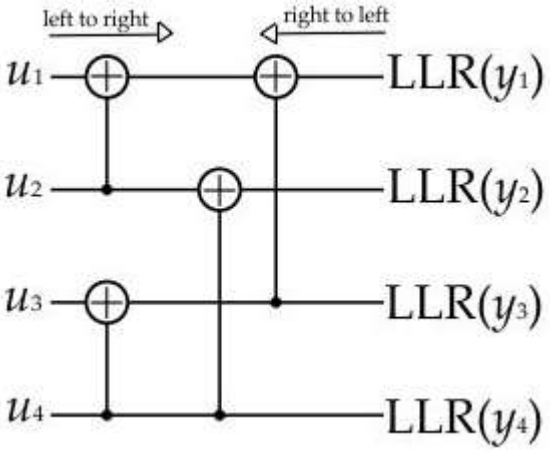

Figure 2a. Basic scheme for Polar Code, for $N = 2$

Figure 2b. Decoding diagram for $N = 4$

Overall framework includes six basic elements:

1. An analysis of the rain image models in order to create a fabricated training dataset 2.
2. Decomposition of the image with the use of a guided filter
3. The architecture of networks consisting of polar encoders and decoders
4.transmit data image in channel
5. Image restoration using image degradation model.
6.calculate bit error rate

With the likelihood ratio value for the number of bit-channel derived from Calculation (1), the method in the decoding goes from right to left following the equivalent technique utilize in the encoding process but in a opposite direction. This possibly will be seen for instance. In Figure 2 when number of message N = 4, where the practice proceeds from left to right. The process of decoding comes to a close with the making of a hard decision, after which the estimated bit ûi is passed from left to right in order to make an intermediate decision.

$$\mathrm{LLR}(y_i) = \log_e \frac{P(y_i|h_i=+1)}{P(y_i|h_i=-1)} = \log_e \frac{\frac{1}{\sigma\sqrt{2\pi}}\exp\frac{-(y_i-1)^2}{2\sigma^2}}{\frac{1}{\sigma\sqrt{2\pi}}\exp\frac{-(y_i+1)^2}{2\sigma^2}} = 2\frac{y_i}{\sigma^2}.$$

Therefore, the most recent bit that was decoded is applied to the estimation of the following bit. In similarity, if the set is calculated incorrectly, that mistake will spread throughout the break of the decoding process and cause further problems.[15]

3. Methodology

Figure 3 depicts a block diagram of communication system is used in this paper that is utilized for the purpose of transmitting raining images over the AWGN channel.

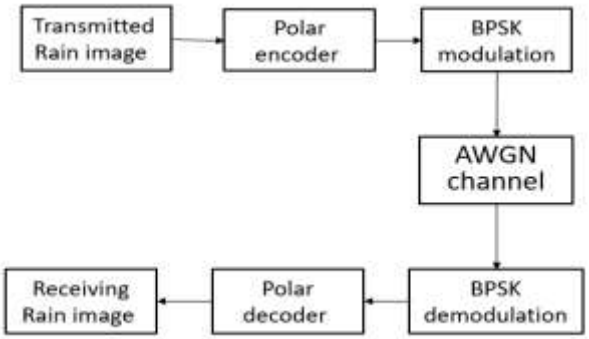

Figure 3 is a block diagram that is currently being considered used in this paper

In order to study the bit error rate of *transmitted* raining images when the successive cancellation decoder and the successive cancellation list decodor are proposed, however the block lengths of polarcodes with of Number of message with 512,1024,2048, and 4096 are utilized at a

fixed – rate of R = 0.5. This rate is maintained throughout the investigation. Lena, Peppers, and Cameraman are the three images that are utilized for simulations. Each of these images has 256 width and 256 length and 8 bits per pixel however is was using different format. The successive-cancelation decoder be able to think of as a special instance of the successive cancelation list decoder [15], in which there is only one possible path. The Successive Cancelation List decoder analyzes L potential pathways, L ≥ 2. When a choice ûi involving a non-frozen bit is taken, the decoder is presented with a new path to take into consideration. When there is a split in a path, the number of possible routes doubles, and when the SCL decoder reaches the limit of 2L, it discards the route that is less likely to occur. This procedure will continue until a determination is made regarding the final bit, at which point the SCL decoder will select the best possible route as the sequence of ûi expected the data bits.[16]

Figure 4. Original images having different format transmit over AWGN channel

Figure 4 provides an illustration of the original photos that were discussed before. The bits that make up the pixels of an image array that can be format the raining image are changed. Every K bits contribute to the generation of the vecctor u with lngth codewords, where codewords bits represent frozen data. Following the creation of the vector u, it is then passed through the polar encoder in order to produce the length of message codeword is x however after being modulated using BPSK, the codeword x is then eventually transmitted through an AWGN channel.

4-Computer Simulation Results

Now, the results of the simulation will be reported for the picture transmission scheme that is depicted in figure 3. The peak signal-to-noise ratio values of the reconstructed raining images are used to evaluate the images' quality across a spectrum of SNR values and block lengths massage. These values are evaluated for a variety of values. Figures 5 and 6 show the results, which are reported in terms of peak signal to noise ratio versus snr values for various code block lengths of codewords with successive cancelation list decoding with list equal to 2 , 4,and 8 however Due to the valuesPSNR versus different SNR curves for rainimage was obtainable in Figurer five however one notes since the value best of the decoded rainimage, in terms of peak signal to noise ratio peak signal to noise ratio PSNR however increases with the length of message N and SC decoders with SNR bigger than 1.3 d_B. And polar decoders successive cancelation or successive cancelation list with L =2 ,4, and 8.These metrics were developed by the authors of the the peak signal to noise ratio value, expressed in decibels, can be calculated as

$$PSNR = 10log_{10}(\frac{size^2}{MSE})$$

And MSE can be represented by

$$MSE = \frac{1}{VB}\sum_{I=1}^{V}\sum_{J=1}^{B}[g(I,J) - g'(I,J)]^2$$

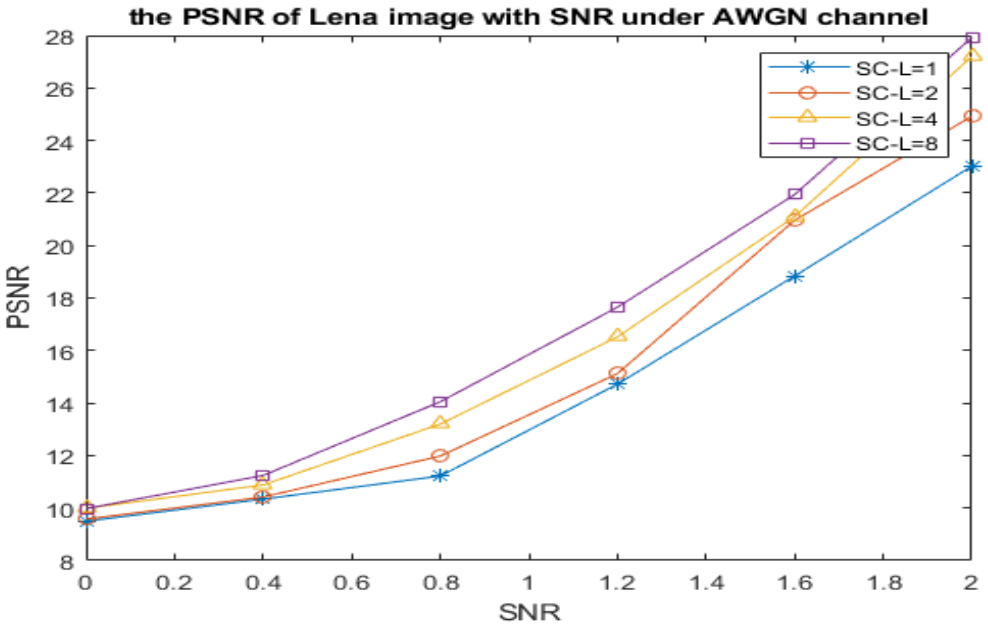

Figure 5a. SNR VS PSNR versus for Lina-rain image N=512

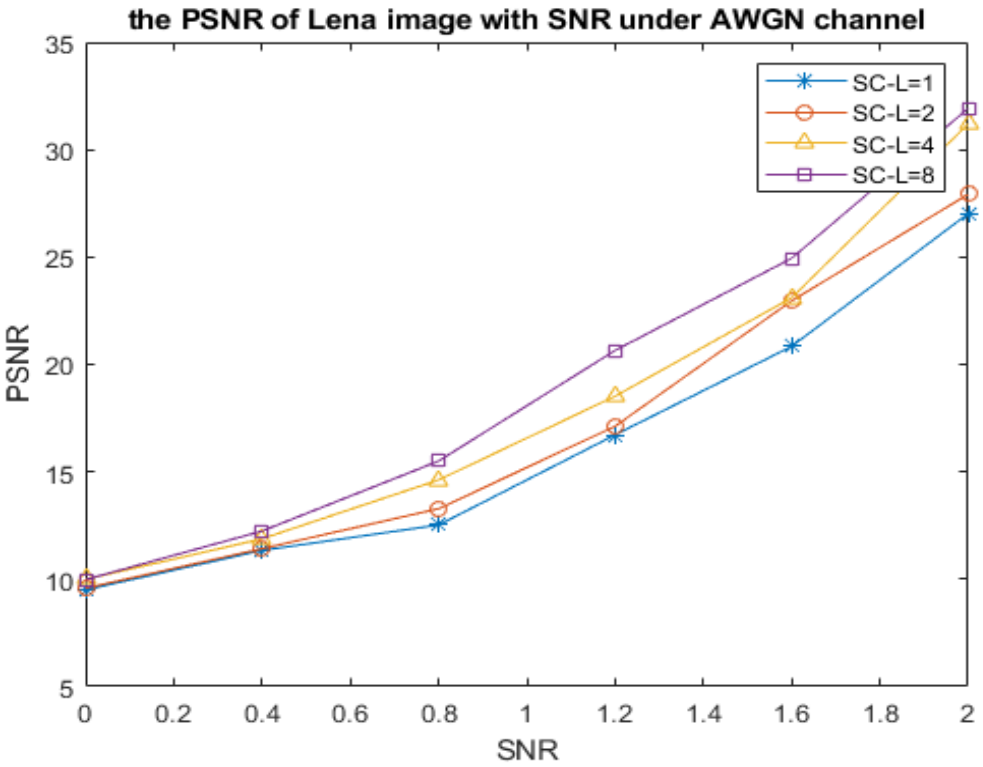

Figure 5b. SNR VS PSNR for Lena-rain image N=1024

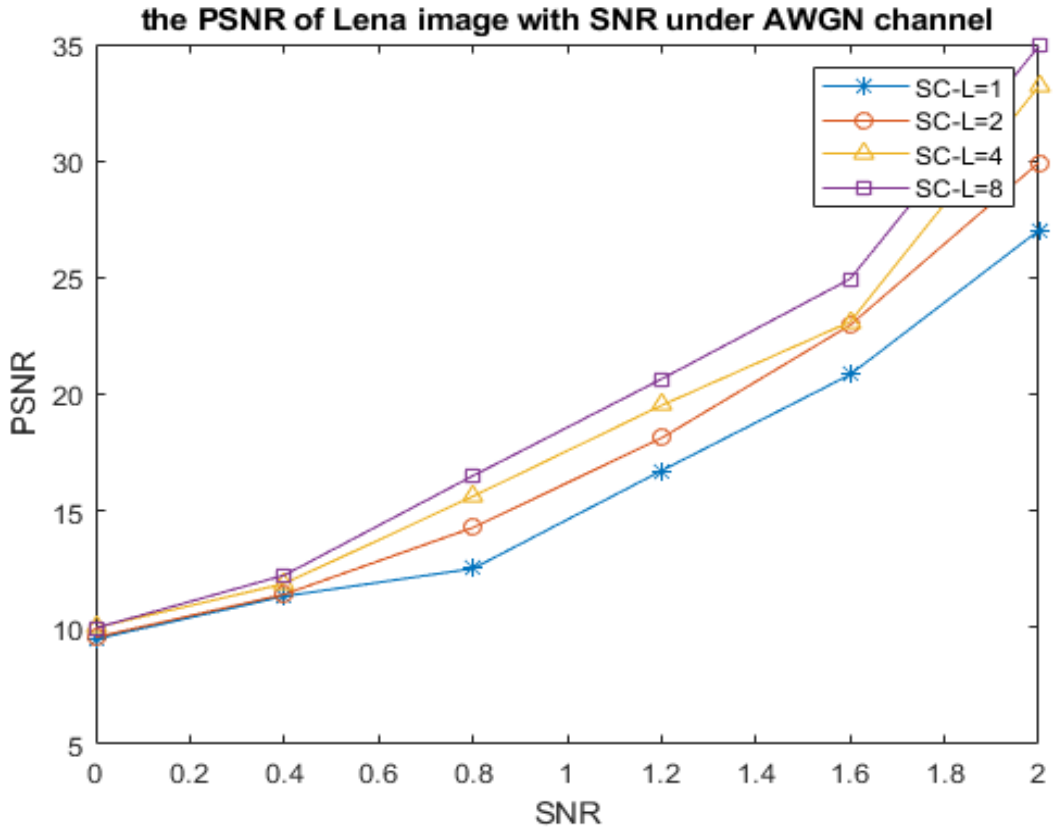

Figure 5c. SNR VS PSNR for Lena-rain image N=2048

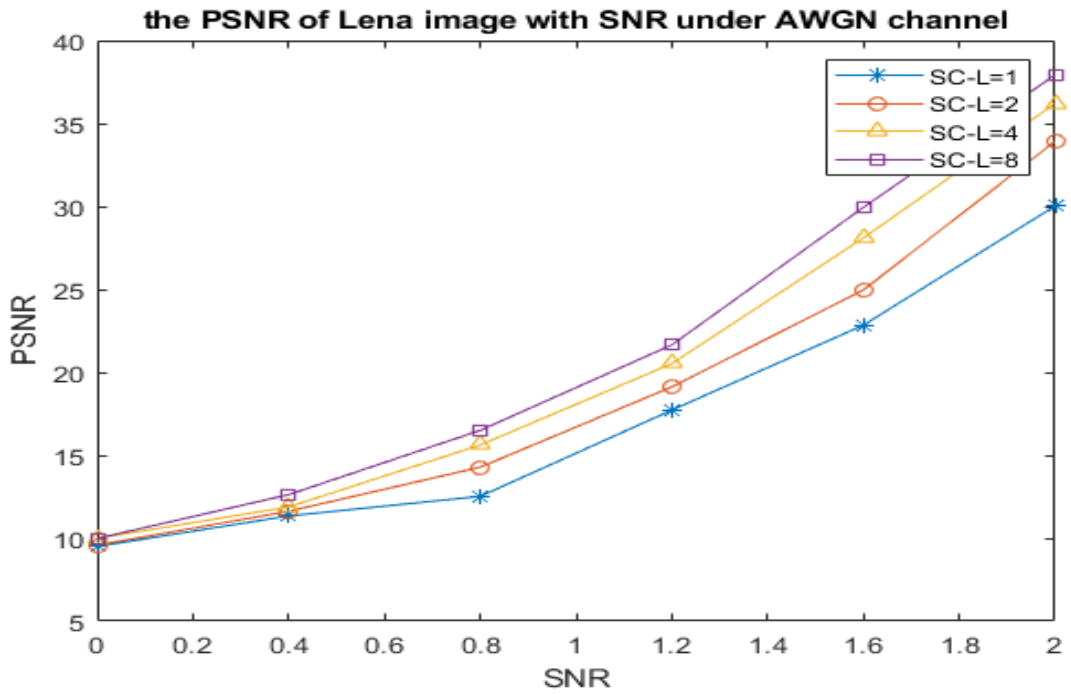

Figure 5d. SNR VS PSNR for Lena-rain image N=4096

Figure 5. peak signal to noise ratio in dB versus SNR for Lena image-rain using successive cancelation decoding for different values of number of pattrens (a) N=512,(b) N=1024, (c) 2048 (d) 4096

Successive cancelation list decoding with L = 2, successive cancelation list decoding with list equal four, and successive cancelation list decoding with list equal eight all exhibit an increase in peak signal to noise ratio with increasing N for SNR values that are more than nearby 1.3 and 1.1 and 1.2 dB, The channel polarization effect is responsible for increment of PSNR that occurs with increasing length message-N. This is how the end product works. Definitely, the number of good bit-channels, or channels that are available to transfer information, will rise proportionally to the block length. As a consequence of this, a better Bhatacharyya factor will be found, which will result in a lower chance of bit errors.

After the image has been reconstructed, the peak signal to noise ratio (peak signal to noise ratio) are used to calculate the decoding enactment for a range of SNR values, where S denotes the energy per bit and No is the density spectral of noise, for N = 512, 1024, 2048, and 4096. Quality of image is termed by PSNR is decoded and the improvements that may be seen as a result of aggregate the number of routes L can be seen in Fig. 6. Visual analysis of the rainimage presented in Figure 6 reveals that the subjective-equality of the decoded rainimage develops with increasing levels of L when the Lenarains image is considered at an SNR value of 1.6. Certainly, as L increases and number of code length is distracting that remain in the decodes rainimage reduces. The theory that raising L causes an improvement in image quality is supported by the fact that PSNR both increase as L increases.

Figure 7 shows the performance of the Peppers picture when SNR is 1.6 dB, and Figure 8c shows the performance of the Cameraman image when SNR is 1.6 dB. Both figures exhibit the same behavior. One can see in Fig. 8 that a rise in L from 4 to 8 results in an increase in PSNR from 25.12 until 27.39 dB. An raising in L from 4 to 8 results in with regard to the image in Figure 6.

Figure 7. remove noise and rain image at receiver

For the rain images, the values of peak signal to noise ratio rises are shown in Tables 1 through 4 for a variety of SNRratios, utilizing either successive cancellation list decoding for $L = 2, 4,$ and 8 for N is equal 512, 1024, 2048, and 4096. These data are presented using successive cancellation list decoding. As can be seen in Table 1, when compared to successive cancellation list decoding decoding,
successive cancellation list decoding with either with list is 2,4,and 8 yields superior peak signal to noise ratio rises results across the board, regardless of the SNR value or the value of N. This holds true regardless of the value of N. the peak signal to noise ratio rises when L is increased when SNR is less than 0.4 dB and cancellation list decoding is used. As an illustration, when SNR is equal to 1.2 dB and N is equal to 4096, the values for peak signal to noise ratio are 15.76 , 18.13 and 19.45 dB, respectively, for List is 2, 4, and 8, individually.

5. Conclusion

Transmitting data over an AWGN network with little SNR ratios. This was accomplished using polar codes used SC and SCL with different list been demonstrated to be reliable for use in environments with low signal-to-noise ratios all rain images. The benefit of utilizing the successive cancellation list decoding algorithm with list equals 2, 4 and 8 rather than the successive cancellation decoding algorithm was validated in all of the scenarios that were tested. For$SNR = 0.9$ dB, the decoding rain image quality improved, but to increase the improvements became less significant as List increased. It is suggested that, in future work, an investigation into the performance of using fast and simplified

successive cancellation list decoding or using another technique for decoding as belief propagation decoding, for example be used to exchange successive cancellation decoding and successive cancellation list. This is for the sake of completeness, so that the topic can be covered in its entirety.

Reference

1. Y. Ding, M. Li, T. Yan, F. Zhang, Y. Liu and R. W. H. Lau, "Rain Streak Removal From Light Field Images," in *IEEE Transactions on Circuits and Systems for Video Technology*, vol. 32, no. 2, pp. 467-482, Feb. 2022, doi: 10.1109/TCSVT.2021.3063853.
2. Jasim, IB, Bayat, O, Ucan, ON. Concatenation of polar codes with three-dimensional parity check (3D-PC) codes to improve error performance over fading channels. *Int J Commun Syst*.2019;32:e3970.https://doi.org/10.1002/dac.3970
3. K. Jiang *et al.*, "Rain-Free and Residue Hand-in-Hand: A Progressive Coupled Network for Real-Time Image Deraining," in *IEEE Transactions on Image Processing*, vol. 30, pp. 7404-7418, 2021, doi: 10.1109/TIP.2021.3102504.
4. K. Lay and H. Huang, "Digital Image Transmission with Polar Codes and Median Filtering," *2019 4th International Conference on Intelligent Green Building and Smart Grid (IGBSG)*, 2019, pp. 371-375, doi: 10.1109/IGBSG.2019.8886247.
5. Yang, X.; Li, H.; Fan, Y.L.; Chen, R. Single Image Haze Removal via Region Detection Network. IEEE Trans. Multimed. 2019, 21, 2545–2560. [CrossRef] IEEE International Conference on Image Processing, Melbourne, Australia, 15–18 September 2013; pp. 914–917.
6. X. Fu, J. Huang, D. Zeng, Y. Huang, X. Ding and J. Paisley, "Removing Rain from Single Images via a Deep Detail Network," *2017 IEEE Conference on Computer Vision and Pattern Recognition (CVPR)*, 2017, pp. 1715-1723, doi: 10.1109/CVPR.2017.186.
7. J. He, L. Yu and W. Yang, "Image De-Raining Via RDL: When Reweighted Convolutional Sparse Coding Meets Deep Learning," *ICASSP 2020 - 2020 IEEE International Conference on Acoustics, Speech and Signal Processing (ICASSP)*, 2020, pp. 2548-2552, doi: 10.1109/ICASSP40776.2020.9052926.
[8] Fu, X.; Huang, J.; Ding, X.; Liao, Y.; Paisley, J. Clearing the skies: A deep network architecture for single-image rain removal. IEEE Trans. Image Process. 2017, 26, 2944–2956.
8. Fu, X.; Huang, J.; Zeng, D.; Huang, Y.; Ding, X.; Paisley, J. Removing rain from single images via a deep detail network. In Proceedings of the IEEE Conference on Computer Vision and Pattern Recognition, Honolulu, HI, USA, 21–26 July 2017; pp. 3855–3863.
9. Fu, X.; Huang, J.; Zeng, D.; Huang, Y.; Ding, X.; Paisley, J. Removing rain from single images via a deep detail network. In Proceedings of the IEEE Conference on Computer Vision and Pattern Recognition, Honolulu, HI, USA, 21–26 July 2017; pp. 3855–3863.
10. C. Tan, J. Chen and L. Chau, "Edge-preserving rain removal for light field images based on RPCA," *2017 22nd International Conference on Digital Signal Processing (DSP)*, 2017, pp. 1-5, doi: 10.1109/ICDSP.2017.8096066.
11. Zhu, Q.; Mai, J.; Shao, L. A fast single image haze removal algorithm using color attenuation prior. IEEE Trans. Image Process.2015, 24, 3522–3533.
12. Hanhart, P., Bernardo, M. V., Pereira, M., G. Pinheiro, A. M., & Ebrahimi, T. (2015). Benchmarking of objective quality metrics for HDR image quality assessment. EURASIP Journal on Image and Video Processing(1), 2015:39. doi: 10.1186/s13640-015-0091-4
13. Ren,W.; Liu, S.; Zhang, H.; Pan, J.; Cao, X.; Yang, M.H. Single image dehazing via multi-scale convolutional neural networks. In Proceedings of the European Conference on Computer

Vision, Amsterdam, The Netherlands, 11–14 October 2016; pp. 154–169.

14. E. Arikan "Channel combining and splitting for cutoff rate improvement," IEEE Trans. Inf. Theory, vol. 52, no. 2, pp. 628–639, Feb. 2006. J. Jin, H.-M. Oh, S. Choi, J. Seo, and J.-J. Lee, "Performance of polar codes with successive cancellation decoding over PLC channels," in Proc. IEEE International Symposium on Power Line Communications and its Applications (ISPLC), Mar. 2015, pp. 24–28.
15. Tal, and A. Vardy, "List decoding of polar codes", IEEE Trans. Inf. Theory, vol. 61, no. 5 pp. 2213–2226, May 2015.